

Hydrogen therapy attenuates irradiation-induced lung damage by reducing oxidative stress

Yasuhiro Terasaki,¹ Ikuroh Ohsawa,² Mika Terasaki,¹ Mikiko Takahashi,¹ Shinobu Kunugi,¹ Kang Dedong,¹ Hirokazu Urushiyama,¹ Shunsuke Amenomori,¹ Mayuko Kaneko-Togashi,¹ Naomi Kuwahara,¹ Arimi Ishikawa,¹ Naomi Kamimura,³ Shigeo Ohta,³ and Yuh Fukuda¹

¹Department of Analytic Human Pathology, Nippon Medical School, Tokyo; ²Environmental Gerontology, Tokyo Metropolitan Institute of Gerontology, Tokyo, Japan; ³Department of Biochemistry and Cell Biology, Institute of Development and Aging Sciences, Graduate School of Medicine, Nippon Medical School, Kawasaki City, Japan

Submitted 12 January 2011; accepted in final form 20 June 2011

Terasaki Y, Ohsawa I, Terasaki M, Takahashi M, Kunugi S, Dedong K, Urushiyama H, Amenomori S, Kaneko-Togashi M, Kuwahara N, Ishikawa A, Kamimura N, Ohta S, Fukuda Y. Hydrogen therapy attenuates irradiation-induced lung damage by reducing oxidative stress. *Am J Physiol Lung Cell Mol Physiol* 301: L415–L426, 2011. First published July 15, 2011; doi:10.1152/ajplung.00008.2011.—Molecular hydrogen (H₂) is an efficient antioxidant that diffuses rapidly across cell membranes, reduces reactive oxygen species (ROS), such as hydroxyl radicals and peroxynitrite, and suppresses oxidative stress-induced injury in several organs. ROS have been implicated in radiation-induced damage to lungs. Because prompt elimination of irradiation-induced ROS should protect lung tissue from damaging effects of irradiation, we investigated the possibility that H₂ could serve as a radioprotector in the lung. Cells of the human lung epithelial cell line A549 received 10 Gy irradiation with or without H₂ treatment via H₂-rich PBS or medium. We studied the possible radioprotective effects of H₂ by analyzing ROS and cell damage. Also, C57BL/6J female mice received 15 Gy irradiation to the thorax. Treatment groups inhaled 3% H₂ gas and drank H₂-enriched water. We evaluated acute and late-irradiation lung damage after H₂ treatment. H₂ reduced the amount of irradiation-induced ROS in A549 cells, as shown by electron spin resonance and fluorescent indicator signals. H₂ also reduced cell damage, measured as levels of oxidative stress and apoptotic markers, and improved cell viability. Within 1 wk after whole thorax irradiation, immunohistochemistry and immunoblotting showed that H₂ treatment reduced oxidative stress and apoptosis, measures of acute damage, in the lungs of mice. At 5 mo after irradiation, chest computed tomography, Ashcroft scores, and type III collagen deposition demonstrated that H₂ treatment reduced lung fibrosis (late damage). This study thus demonstrated that H₂ treatment is valuable for protection against irradiation lung damage with no known toxicity.

apoptosis; reactive oxygen species; hydroxyl radical; peroxynitrite; free radical scavengers; radioprotector

BODY IRRADIATION IS OFTEN used for conditioning before bone marrow transplantation because it has immunosuppressive effects on host immune systems, which minimizes the risk of engraftment failure (7). Pulmonary complications of bone marrow transplantation cause significant morbidity and mortality. Interstitial pneumonitis, which is a radiation-induced lung injury, has a reported incidence of 10–84% after total body irradiation (47). The lung is one of the organs most susceptible to radiation injury (34), and development of inter-

stitial pneumonitis increases according to radiation dose, especially single-fraction total body irradiation at higher dose rates (9) and higher total lung doses (3, 37).

Ionizing radiation interacts with water molecules in biological systems and produces various reactive oxygen species (ROS) and reactive nitrogen species (RNS), which can cause cell damage and even cell death (41). An estimated 60–70% of ionizing radiation-induced cell injury was reportedly caused by hydroxyl radicals ($\cdot\text{OH}$) (36, 46, 51), which react rapidly with cellular macromolecules to damage DNA, lipids, and proteins. The lung is an organ that is extremely susceptible to the harmful effects of irradiation (34), and irradiation-induced lung injury is reported to be initiated and sustained by oxidative stress (10, 22, 24). Therefore, prompt elimination of irradiation-induced ROS should protect lung tissue from the damaging effects of irradiation. In fact, ROS scavengers have been documented to reduce oxidative lung injury resulting from ionizing radiation (38, 39). However, no ideal radioprotectant, with the desired effectiveness, toxicity, selectivity, and tolerance, has yet been discovered.

Molecular hydrogen (H₂) was recently reported to be a novel antioxidant and has the potential to be widely used in medical applications as safe and effective with no known side effects. H₂ also possesses certain unique properties, such as being able to quench injurious ROS, $\cdot\text{OH}$, and peroxynitrite (ONOO[−]), while preserving the metabolic oxidation-reduction reaction and other less potent ROS such as hydrogen peroxide (H₂O₂) and superoxide radical (O₂^{•−}) (32). H₂ can also penetrate cell membranes and can easily target organelles, including mitochondria and nuclei (32). In addition, H₂ suppressed oxidative stress-induced injury in several organs; reduced ischemia-reperfusion injury in the brain (32), heart (16), liver (12), and retina (31); and protected against nephrotoxicity (29). A recent report demonstrated that H₂ treatment also suppressed radiation-induced acute injury in lymphocytes and intestinal crypt cells but did not include analysis of the molecular mechanism of H₂-rich PBS as an ROS scavenger in vitro or analysis of the suppression, by one intraperitoneal injection of H₂-rich saline, of late irradiation damage in mice in vivo (35). In the present study, which focuses on the lung, we investigated whether H₂ treatment exerted radioprotective effects, with the study evaluating the mechanism of action of H₂-rich PBS or media as an efficient ROS scavenger in vitro and the suppression of both acute damage and late fibrotic changes in vivo. The in vitro analysis included use of electron spin resonance (ESR) and 2-[6-(4'-hydroxy) phenoxy-3H-xanthen-3-on-9-yl]benzoate (HPF) signals. The in vivo experiments utilized inhalation of

Address for reprint requests and other correspondence: Y. Terasaki, Dept. of Analytic Human Pathology, Graduate School of Medicine, Nippon Medical School, 1-1-5 Sendagi, Bunkyo-ku, Tokyo 113-8602, Japan (e-mail: terasaki@nms.ac.jp).

H₂ gas and drinking of H₂-rich water as H₂ treatment. Our results demonstrate that treatment with H₂, as an antioxidant, protected cultured lung epithelial cells and lungs of mice from irradiation-induced interstitial pneumonitis.

MATERIALS AND METHODS

Production of H₂-rich PBS and medium. To make H₂-rich Dulbecco's PBS (Invitrogen, Carlsbad, CA) or culture medium, for 20 min we bubbled H₂ mixed with air (both at 1 l/min) to saturation (H₂/air: 50/50 vol%) into 100 ml of PBS or phenol red-free RPMI medium 1640 (Invitrogen) containing 1% penicillin-streptomycin. We also prepared control N₂-rich PBS or medium lacking H₂ by bubbling N₂ mixed with air (both at 1 l/min) to saturation (N₂/air: 50/50 vol%) into 100 ml of PBS or medium during 20 min. We put H₂-rich PBS or medium into culture flasks and confirmed, via a needle-type H₂ sensor (Unisense, Aarhus, Denmark), an H₂ concentration of more than 0.3 mM. The oxygen level, as measured by a needle-type O₂ sensor (Unisense), was about 0.12 mM in both H₂-enriched and N₂-enriched solutions. The pH level, as measured by a B-213 Twin Compact Meter (HORIBA, Kyoto, Japan), was between 7.4 and 8.0 in both H₂-enriched and N₂-enriched solutions.

Cell culture and H₂ treatment. Human lung epithelial cell line A549 cells were obtained from the Cell Research Center for Biomedical Research (Institute of Development, Aging and Cancer, Tohoku University) and were grown in culture dishes or culture slides with maintenance medium containing 10% FBS and 1% penicillin-streptomycin in a 5% CO₂ humidified chamber. For radioprotective studies, we removed medium, treated A549 cells with H₂-rich or N₂-rich PBS or medium in culture dishes or culture slides in tightly closed containers filled with H₂-rich or N₂-rich mixed gases as described above, and then immediately exposed cells to 10 Gy irradiation via an X-ray generator (150 kVp, 5 mA; Hitachi Medical, Tokyo, Japan).

ESR studies of radioprotective H₂ treatment. We used 5,5-dimethyl-1-pyrroline N-oxide (DMPO; Labotec, Tokyo, Japan) to trap free radicals, especially ·OH, and detected ESR signals after irradiation via an ESR spectrometer (JES-RE3; JEOL, Tokyo, Japan). As a standard of the reaction of ·OH with DMPO, we produced ·OH by means of the Fenton reaction with the mixture of 0.1 mM H₂O₂ and 1 mM FeCl₂ in the presence of 0.1 mM DMPO and obtained ESR measurements of the solution. We normalized the sensitivity of each experiment with the strength of the internal ESR signal derived from Mn²⁺, as shown by M in Fig. 1, A and B. For radioprotective studies, we prepared H₂-rich or N₂-rich medium in culture dishes in tightly closed containers filled with gases as described, added 0.1 mM DMPO, and immediately exposed each flask to 10 Gy irradiation. Ten minutes after irradiation, we detected ESR signals of ·OH in irradiated media by using flat cuvettes (Labotec). A differential spectrum was obtained by digitally subtracting one spectrum from another to visualize signals reduced by H₂. The heights N₂-h and H₂-h in Fig. 1C reflect signal intensities. Comparison of the ratios of heights of N₂-h to M and H₂-h to M appears in Fig. 1D (n = 6 experiments).

Detection of irradiation-induced ·OH and ONOO⁻ by fluorescent indicators. To detect cellular ·OH and ONOO⁻, after removal of maintenance medium, we treated A549 cells with H₂-rich or N₂-rich medium and added 5 μM HPF (Daiichi Pure Chemicals, Tokyo, Japan) and 5 μM Hoechst 33342 dye (Invitrogen; nuclei stained as blue), after which we immediately exposed cells to 10 Gy irradiation and incubated them in culture slides in tightly closed containers filled with H₂-rich or N₂-rich mixed gases as described. After 15 min of incubation, we replaced the medium with H₂-rich or N₂-rich PBS plus 5 μM HPF and 5 μM Hoechst 33342 dye and continued the incubation for 15 min in tightly closed containers filled with H₂-rich or N₂-rich mixed gases. We visualized signals via a filter set for FITC and 4',6-diamidino-2-phenylindole (DAPI; Vector Laboratories, Burlingame, CA), with an inverted microscope (Eclipse TE2000-E; Nikon, Tokyo, Japan). We obtained images by use of a digital camera

and the software MetaMorph (Molecular Devices, Downingtown, PA), with constant camera exposure settings throughout. HPF can be oxidized by ·OH, ONOO⁻, and lipid peroxides but not H₂O₂, nitric oxide radical, or O₂^{·-} (43). We quantified fluorescent signals for 100 cells from each experiment by using an image analysis system (MacScoop version 2.5; Mitani, Fukui, Japan, and NIH Image software).

Detection of cell damage after irradiation. At 36 h of incubation (30, 40) after 10 Gy irradiation in tightly closed containers filled with H₂-rich or N₂-rich mixed gases, we assessed A549 cell survival by manually counting the cells, double-stained with 1 μM propidium iodide (Invitrogen; nuclei of dead cells stained pink) and 5 μM Hoechst 33342 dye (Invitrogen; nuclei of both dead and living cells stained blue), in closed flasks in N₂-rich (H₂⁻) or H₂-rich (H₂⁺) medium.

Antibodies. Antibodies were purchased for transforming growth factor-β1 (TGF-β1) and Bax (Santa Cruz Biotechnology, Santa Cruz, CA), porin (Merck KGaA, Darmstadt, Germany), type III collagen (SouthernBiotech, Birmingham, AL), active caspase 3 (Abcam, Cambridge, MA), caspase 3 (Cell Signaling Technology, Danvers, MA), 4-hydroxy-2-nonenal (4-HNE) and 8-hydroxydeoxyguanosine (8-OH-dG) (Nikken Seil, Tokyo, Japan), and GAPDH (Epitomics, Burlingame, CA). Mouse monoclonal antibodies against Bcl-x_L and Bcl-2 were prepared as described previously (27).

Immunocytochemistry. A549 cells were grown in eight-well culture slides (BD Biosciences, Sparks, MD). All procedures were performed at room temperature. At 24 h of incubation (30, 40) after 10 Gy irradiation in a tightly closed container filled with H₂-rich or N₂-rich mixed gases, cells were incubated with MitoTracker Red CMXRos (Invitrogen) for 15 min before fixation with 4% paraformaldehyde in Sorensen's phosphate buffer (0.15 M, pH 7.4; Electron Microscopy Sciences, Hatfield, PA). Cells were washed with PBS, permeabilized for 10 min with 0.1% Triton X-100 in PBS, washed with PBS, and incubated for 20 min with blocking buffer (5% goat serum in PBS). Cells were then washed with PBS and incubated with antibody-anti-8-OH-dG at 5 μg/ml, or anti-4-HNE at 25 μg/ml, or anti-Bax at 2 μg/ml for 3 h, washed with PBS, and incubated for 1 h with FITC-labeled goat anti-mouse or anti-rabbit IgG (Zymed, San Francisco, CA). After samples were washed with PBS, nuclei were counterstained with DAPI (Vector Laboratories). Signals were visualized via a filter set for FITC, with an upright microscope (BX60; Olympus, Tokyo, Japan). Images were obtained by using an Olympus DP70 digital camera and software (Olympus), with constant camera exposure settings throughout. Fluorescent signals in response to 8-OH-dG or 4-HNE were quantified for 100 cells from each experiment by using an image analysis system (MacScoop version 2.5 and NIH Image software). A confocal laser-scanning microscope (TCS-SP5; Leica Microsystems, Mannheim, Germany) based on an upright microscope (DM6000B; Leica Microsystems) equipped with a 405 diode/argon/HeNe 543/HeNe 633 laser was also used for Bax translocation images.

Hydrogen-rich water administration. H₂ was dissolved in water under high pressure (0.4 MPa) to a supersaturated level by using a hydrogen water-producing apparatus (version 2) produced by Blue Mercury (Tokyo, Japan). The saturated hydrogen water was prepared every week and stored in an aluminum bag with a concentration of more than 0.6 mM. Each day, the hydrogen water in the aluminum bag was placed into a closed glass vessel (70 ml) equipped with an outlet line containing two ball bearings, which kept the water from being degassed. This vessel ensured a hydrogen concentration of more than 0.4 mM after 1 day. Hydrogen water degassed by gentle stirring was used for control animals; complete removal of gas was confirmed with a needle-type H₂ sensor (Unisense).

Irradiation lung injury mouse model. Fibrosis-prone mice (female C57BL/6J, 8 wk old, approximate body weight 20 g; Sankyo Labo Service, Tokyo, Japan) were used. Animal protocols were approved by the Animal Care and Use Committee of Nippon Medical School.

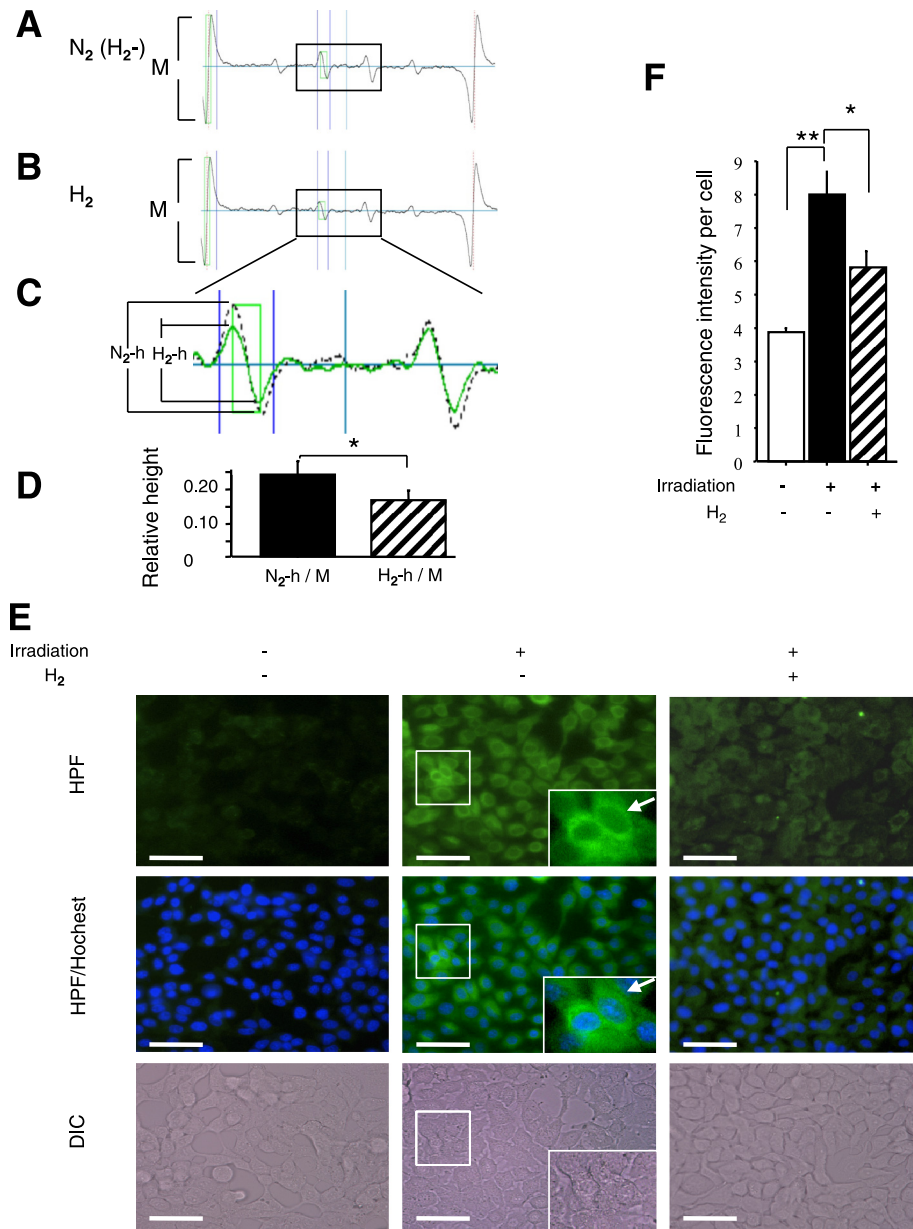


Fig. 1. Reduction by H_2 of irradiation-induced $\cdot OH$ in media and cultured cells. **A** and **B**: spin trap 5,5-dimethyl-1-pyrroline *N*-oxide (DMPO) was used to obtain electron spin resonance (ESR) signals of the DMPO- $\cdot OH$ radical from N_2 -rich (H_2^-) (**A**) or H_2 -rich (H_2^+) (**B**) RPMI medium in tightly closed containers. M (**A**, **B**) is the strength of the internal ESR signal derived from Mn^{2+} for normalization. **C**: merged view of the black rectangles in **A** and **B**. Heights of N_2-h and H_2-h reflect the signal intensity of DMPO- $\cdot OH$ derived from irradiation-induced $\cdot OH$. **D**: comparison of ratios of the heights of N_2-h to M and H_2-h to M ($n = 6$ experiments). **E**: representative images of fluorescence of the reactive oxygen species ($\cdot OH$ and $ONOO^-$) marker 2-[6-(4'-hydroxy)phenoxy-3*H*-xanthen-3-on-9-yl]benzoate (HPF) with Hoechst 33342 dye (for nuclei) and differential interference contrast (DIC) microscopy, taken 30 min after irradiation. *Insets*: high-magnification views of the areas in the rectangles. Arrows indicate increased HPF signals in cytoplasmic regions. Scale bars = 50 μm . **F**: HPF fluorescence in cells treated with 10 Gy irradiation in N_2 -rich (H_2^-) or H_2 -rich (H_2^+) PBS was quantified for 100 cells ($n = 5$). Data represent means \pm SE. * $P < 0.05$ and ** $P < 0.01$.

The mice were housed five per cage and kept under standard laboratory conditions, during which food and water were supplied ad libitum. Mice were randomly distributed into three groups: 1) control (sham-irradiated), 2) irradiation without H_2 treatment [with mixed N_2 gas (3% N_2 and 97% air) and no H_2 -rich water], and 3) irradiation with H_2 treatment [with mixed H_2 gas (3% H_2 and 97% air) and H_2 -rich water]. The whole lung of each mouse was irradiated with a single dose of 15 Gy, 150 kVp X-rays at 0.5 Gy/min. Lead strips shielded the head, abdomen, and extremities. Mice were anesthetized before irradiation with an intraperitoneal injection of pentobarbital sodium (40 mg/kg). Mice were treated with mixed gas (3% H_2 and 97% air or 3% N_2 and 97% air) supplied through a vaporizer utilizing facemasks and gas flow meters (H_2 or N_2 : 0.3 l/min, air: 9.7 l/min). The H_2 concentration in the mixed gas was determined via a gas chromatograph (Model TGA-2000; Teramecs, Kyoto, Japan). Treatment groups inhaled 3% H_2 or 3% N_2 for 90 min during the 30-min irradiation period and 60-min recovery period and drank water with or without H_2 -rich water ad libitum after the irradiation phase until evaluation. Subgroups were evaluated at 1, 3, and 7 days and 5 mo

after irradiation for acute and late irradiation lung damage. On selected days after irradiation, animals were anesthetized and exsanguinated by cutting of the abdominal aorta. The trachea was cannulated, and lungs were removed. The left lungs were immediately frozen at $-80^\circ C$ and later used for malondialdehyde (MDA) and Western blot analyses. The right lungs, which were used for microscopic analyses, were fixed for 8 h at $4^\circ C$ in 4% paraformaldehyde in 0.1 M phosphate buffer (pH 7.4), with an inflation pressure of 20 cm H_2O , after which they were embedded in paraffin.

Histology and fibrosis score. Paraffin-embedded sections were stained with hematoxylin and eosin for routine histological examination and elastica Masson-Goldner (EMG) for evaluation of collagen deposition. Remaining sections of the right lungs were processed for immunohistochemical studies. The severity of lung fibrosis was evaluated via the Ashcroft score, as described previously (2). Briefly, entire fields of 10 sections of the right lung were scanned at a magnification of $\times 100$, and each field was graded visually from 0 (normal) to 8 (total fibrotic obliteration of the field). The mean value of grades obtained for all fields was used as the visual fibrosis score.

Immunohistochemistry. Paraffin-embedded mouse lung sections were deparaffinized. To detect type III collagen, sections were treated with 0.1% pepsin for 15 min at 37°C. After endogenous peroxidase activity and nonspecific binding sites were blocked via the method of Isobe and Brown (4) and use of 5% normal rabbit serum (Vector Laboratories) in PBS, sections were incubated overnight at 4°C with type III collagen antibody at a dilution of 1:40. After sections were washed, they were incubated with horseradish peroxidase (HRP)-conjugated anti-goat antibodies [Histofine Simple Stain MAX PO (G); Nichirei Biosciences, Tokyo, Japan] for 1 h at room temperature and were visualized with 3,3'-diaminobenzidine tetrahydrochloride (DAB; Dojindo Laboratories, Kumamoto, Japan) and H₂O₂. To detect 8-OH-dG, sections were microwaved in DakoCytomation Target Retrieval Solution (Dako, Hamburg, Germany) for 10 min at 100°C, followed by slow cooling and three washings in PBS. After endogenous peroxidase activity was blocked via the method of Isobe and Brown (4), sections were treated with Histofine MOUSESTAIN KIT (Nichirei Biosciences) to prevent reaction of endogenous mouse immunoglobulin in the tissue to anti-mouse HRP-conjugated second antibody, and they were then incubated overnight at 4°C with 8-OH-dG antibody at 5 µg/ml. After sections were washed, they were incubated with HRP-conjugated anti-mouse antibody [Histofine Simple Stain MAX PO (M); Nichirei Biosciences] for 1 h at room temperature and visualized by using 3-amino-9-ethylcarbazole (AEC) + substrate chromogen (Dako). Negative controls were normal goat or mouse IgG; bound peroxidase was detected with DAB or AEC (Dako). Sections were counterstained with Mayer's hematoxylin (Merck, Darmstadt, Germany). The percentage of areas positive for type III collagen per field of view was analyzed in blind fashion for lungs from each group ($n = 6$). The numbers of 8-OH-dG-positive cells per field of view were also counted and analyzed in similar fashion ($n = 6$). Means of positive values were compared with corresponding values for each group via an image analysis system (MacScoop version 2.5).

TUNEL. For in situ analysis of DNA fragmentation, terminal deoxynucleotidyl transferase (TdT) dUTP nick end-labeling (TUNEL) staining was performed with a commercial kit (ApopTag Plus Peroxidase In Situ Apoptosis Detection Kit S7101; Chemicon, Temecula, CA), according to the manufacturer's instructions. In brief, paraffin-embedded lung sections from irradiated mice were deparaffinized, after which they were washed twice with PBS and digested with proteinase K (20 µg/ml) for 7 min, and endogenous peroxidase was then quenched with 3% H₂O₂ for 20 min. After two washings with PBS, sections were incubated with TdT at 37°C for 60 min. This incubation was followed by incubation with anti-digoxigenin-peroxidase for 60 min at room temperature and color development with H₂O₂-DAB for 20 min, followed by three washings in Milli-Q water. The sections were counterstained with Mayer's hematoxylin and covered with coverslips. Omission of TdT from the incubation buffers during processing constituted the technical negative control. The numbers of TUNEL-positive cells per field of view were counted and analyzed in blind fashion for lungs from each group ($n = 6$). Means of positive values were compared with corresponding values for each group via an image analysis system (MacScoop version 2.5).

Western blot analysis. Western blot analysis was performed according to a standard procedure for each experiment. Protein quantification was determined by using the BCA Protein Assay Kit (Thermo Scientific, Rockford, IL). A549 cells or frozen mouse left lung were homogenized in mammalian protein extraction reagent containing a protein-stabilizing cocktail (Halt Protease Inhibitor Cocktail; Thermo Scientific), 150 mM NaCl, and 1 mM EDTA. Mitochondria were isolated from total lung homogenates with use of the Mitochondria Isolation Kit for Tissue (Thermo Scientific) according to the manufacturer's instructions. The mitochondrial fraction was identified on the basis of a high expression of porin. Lysates were centrifuged (12,000 revolution/min, 5 min), and the supernatant was termed lysates. Lysates containing equal amounts of protein were boiled for

5 min in SDS sample buffer, separated with 10% SDS-PAGE, and transferred to polyvinylidene difluoride membranes (Invitrogen) with an electroblot apparatus (Invitrogen). Membranes were incubated for 1 h at room temperature with protein-free T20 Tris-buffered saline (TBS) blocking buffer (Thermo Scientific), and they were then incubated at 4°C for ~16 h with antibodies at a dilution of 1:1,000 against TGF-β1, Bax, Bcl-x_L, active caspase 3, caspase 3, porin, or GAPDH. After membranes were washed several times with TBS containing 0.1% Tween 20 (TBS-T), they were incubated with appropriate HRP-conjugated second antibodies (Promega, Madison, WI) for 45 min, washed with TBS-T, and developed with SuperSignal West Femto Luminol/Enhancer solution (Thermo Scientific). Immunoreactivity on blots was detected with the LAS-4000 Luminescent Image Analyzer with CCD Camera (Fujifilm, Tokyo, Japan) and quantified by means of densitometry with Fuji Image Gauge software (version 4.0; Fujifilm). After proteins were stripped from the blotting membrane by 15 min of incubation in Restore PLUS Western Blot stripping buffer (Thermo Scientific), each protein was quantified after reaction with appropriate antibodies and was expressed as a ratio to the amount of GAPDH protein. Five or six respective results are reported relative to corresponding respective results for no irradiation controls in five or six experiments (no irradiation = 1.0).

MDA assay. Levels of free MDA, a marker of oxidative stress, were determined in lysates of irradiated right lungs in the presence of butylated hydroxytoluene by means of the MDA kit (BIOXYTECH MDA-586; Oxis International, Foster City, CA). Irradiated mice having N₂-rich ($n = 5$) or H₂-rich ($n = 5$) treatment and controls (no irradiation; $n = 5$) were analyzed. Free MDA levels were normalized against protein contents in lysates.

Micro-CT. Micro-computed tomography (micro-CT) of mice was performed with the LCT-100 micro-CT system (LaTheta; Aloka, Tokyo, Japan). The intensity of X-rays in air is -1,000 Hounsfield units (HU), and that in water is 0 HU. CT images were acquired with the X-ray source biased at 50 kVp and 1 mA. Slice thickness was 0.3 mm. Image size was 480 × 480, and the field of view was 48 mm at a resolution of 0.10 mm per pixel. Areas between -400 and -200 HU were said to be areas of abnormal high density for lung field analysis. The ratio of the area of abnormal high density to the whole lung field in the same slice was calculated by LCT-100 system software and was compared for nonirradiated and irradiated mice with or without H₂ treatment (18, 20).

Statistical analysis. For each data set, arithmetic means and standard error of the mean values were calculated, and Student's *t*-test was used to compare paired or independent variables. Statistical differences among groups were determined by using one-way ANOVA. **P* < 0.05 and ***P* < 0.01 were set as statistically significant.

RESULTS

H₂ reduces irradiation-induced 'OH levels in media and in cultured cells. We studied the effects of H₂ on ESR signals to confirm that H₂ can reduce levels of free radical species, especially 'OH induced by irradiation. We produced irradiation-induced 'OH in medium and analyzed 'OH levels by spin-trapping with DMPO. ESR measurements indicated that H₂ did indeed reduce DMPO-OH signals derived from irradiation-induced 'OH in medium (Fig. 1, A–D).

Inasmuch as we confirmed that H₂ reduced irradiation-induced 'OH in culture medium, just as for 'OH produced by the Fenton reaction (32), we next investigated whether H₂ could directly neutralize 'OH induced by irradiation in living cells. A549 cells were irradiated and were assessed for green fluorescence produced by oxidized HPF (a marker of oxidation by 'OH and ONOO⁻) in PBS. Exposure of cells to irradiation in N₂-rich PBS led to increased HPF signals in cytoplasmic

regions of cells (Fig. 1E). H₂ significantly reduced HPF signals with sufficient permeability of cell membranes (Fig. 1, E and F). These results suggest that H₂ can reduce cellular ROS ($\cdot\text{OH}$ and ONOO^-) produced by irradiation in living lung epithelial cells.

H₂ protects cultured cells from damage caused by oxidative stress induced by irradiation. To investigate whether H₂ can effectively protect cells from oxidative stress damage induced by irradiation, we studied the level of oxidative stress and apoptosis with an in vitro irradiation model. After culture medium was replaced with H₂-rich medium, oxidative stress in A549 cells was immediately induced by irradiation. At 24 h after induction of ROS by irradiation, H₂, with sufficient permeability to the cell membrane, seemed to protect cytoplasm from oxidation, as shown by significantly decreased 8-OH-dG levels in irradiated cells (Fig. 2, A and B). Moreover, H₂ also significantly reduced levels of 4-HNE, an end product of lipid peroxides, in cytoplasm of irradiated cells (Fig. 2, C and D), which indicated that it protected lipids from peroxidation. Consistent with these results and others reporting upregulation of Bax and activation of caspase 3 by ionizing irradiation (41), we found, via Western blotting, that H₂ significantly reduced levels of Bax (Fig. 3, A and B) and active caspase 3 (Fig. 3, A and C) as markers of an apoptotic response in lysates of irradiated cells after a 24-h incubation with H₂-rich medium. By means of immunocytochemistry, we confirmed Bax activation induced by irradiation and also confirmed the reduction of it by H₂ treatment, as evidenced by translocation (arrows; yellow color in merged images of Fig. 3D) of Bax (green color) from the cytosol to mitochondria (MitoTracker; red color) (Fig. 3D). We detected clear expression Bcl-x_L in A549 cells that had had no irradiation and reduced levels of Bcl-x_L expression after irradiation. H₂ treatment tended to maintain this reduction although the difference was not statistically different (Fig. 3A). We also confirmed, by manually counting the double-stained cells with a fluorescence microscope at 36 h after irradiation, that H₂ significantly protected cell viability (Fig. 2, E and F).

Taken together, these findings show that H₂ protects in vitro cultured cells against damage from oxidative stress induced by irradiation, as evidenced by reducing the apoptotic response and cell viability.

H₂ protects against irradiation-induced lung damage in mice. To examine the applicability of H₂ treatment in vivo, with H₂ acting as an antioxidant, we used a mouse model of lung injury caused by irradiation to evaluate inhalation of H₂ gas during the irradiation period and drinking H₂-rich water after irradiation. Within 1 wk after irradiation (the acute phase of damage), irradiated mice that had had no H₂ treatment had marked numbers of alveolar cells that were positive for 8-OH-dG and TUNEL staining (markers of oxidative stress and apoptosis, respectively), whereas irradiated mice with H₂ treatment evidenced significantly less staining (Fig. 4, A–D). Consistent with these results, levels of MDA (a marker of lipid peroxidation) (Fig. 4E) and levels of Bax, the profibrotic cytokine TGF- β 1, and Bax mitochondrial translocation (Fig. 4, F–J) were also significantly reduced in lung tissue from irradiated mice after H₂ treatment, when compared with levels for irradiated mice without H₂ treatment.

At 5 mo after irradiation (late damage), chest micro-CT showed that irradiated mice had a regional increase in the amount of radioopaque area indicating lung lesions, whereas

irradiated mice that had had H₂ treatment demonstrated significantly less damage (Fig. 5, A and B). By means of immunohistological analysis, we confirmed that irradiated mice had marked fibrotic changes in alveolar areas, but irradiated mice treated with H₂ demonstrated significantly less damage, as evidenced by EMG staining, Ashcroft scores (Fig. 5, C and D), and type III collagen staining (Fig. 5, E and F). All these results indicate that in vivo H₂ treatment can reduce irradiation-induced oxidative stress and suppress acute damage and subsequent fibrotic damage of lungs in mice after irradiation.

DISCUSSION

In the present study, we investigated whether H₂ treatment exerted a radioprotective effect on the lung. We demonstrated that as an antioxidant, H₂ could protect cultured lung epithelial cells and lungs of mice from irradiation damage (interstitial pneumonitis).

The harmful effects of ionizing radiation have been recognized as resulting from both direct and indirect mechanisms. Direct action damages sensitive molecules in cells, whereas indirect actions occur when ionizing radiation interacts with water molecules in cells, which leads to production of reactive free radicals such as $\cdot\text{OH}$, ONOO^- , $\text{O}_2^{\cdot-}$, and H_2O_2 . The half-lives of these free radicals are extremely short; however, they do immediately react with nearby biomolecules, produce severe site-specific oxidative injury, can disrupt cell function, and may kill cells. $\cdot\text{OH}$ and ONOO^- are the highly reactive products of ROS generated in cells; they react rapidly with cellular macromolecules to damage DNA, lipids, and proteins and exert strong cytotoxic effects. $\cdot\text{OH}$ has been estimated to cause 60–70% of ionizing radiation-induced cell damage (36, 46, 51).

Recent studies demonstrated that H₂ reduced $\cdot\text{OH}$ and ONOO^- and may have potential for wide use in medical applications as a novel, safe, effective antioxidant with minimal side effects (12, 16, 29, 31, 32, 35). Elimination of $\cdot\text{OH}$ is biologically important, because although $\text{O}_2^{\cdot-}$ and H_2O_2 are detoxified by the antioxidant defense enzymes superoxide dismutase (SOD) ($\text{O}_2^{\cdot-}$) and peroxidase or glutathione peroxidase (H_2O_2), no enzyme detoxifies $\cdot\text{OH}$. Because $\cdot\text{OH}$ and ONOO^- are injurious ROS and produce most of the ionizing radiation-induced acute damage (36, 46, 51), we hypothesized that H₂ treatment may be radioprotective as a result of its ROS-scavenging effects.

In this study, we successfully detected, via ESR, irradiation-induced $\cdot\text{OH}$, and we reduced its signal level by using H₂ (Fig. 1, A–D). We also found that irradiation enhanced ROS ($\cdot\text{OH}$ and ONOO^-) accumulation, as evidenced by HPF signals in cells, and that H₂ reduced this irradiation effect (Fig. 1, E and F). These results are consistent with a previous report in which H₂ reduced both the DMPO-OH signals derived from $\cdot\text{OH}$ produced by the cellular Fenton reaction and the HPF signal as $\cdot\text{OH}$ in living cells after induction by a mitochondrial respiratory complex III inhibitor (32). Although $\cdot\text{OH}$ rapidly reacts with cellular macromolecules to damage DNA, lipids, and proteins, we indeed obtained direct evidence that our H₂ treatment scavenged $\cdot\text{OH}$ produced by irradiation in vitro as well as $\cdot\text{OH}$ produced by the cellular Fenton reaction in vitro (32).

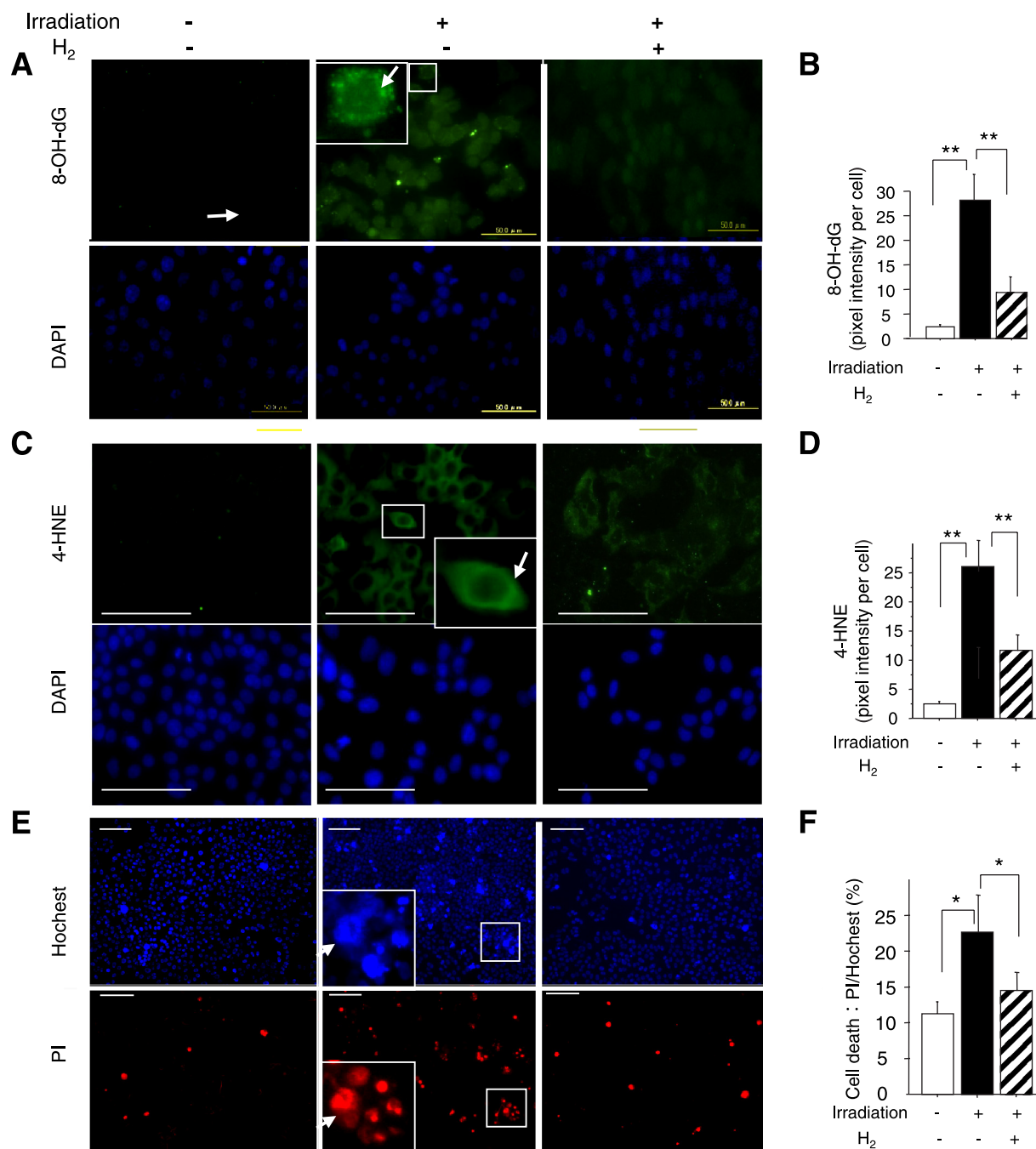


Fig. 2. Reduction of irradiation-induced oxidative stress and protection of irradiated cultured cells by H₂. After removal of maintenance medium, cells were incubated in N₂-rich (H₂⁻) or H₂-rich (H₂⁺) medium in tightly closed containers and were immediately exposed to 10 Gy irradiation. A and C: cells were maintained in N₂-rich (H₂⁻) or H₂-rich (H₂⁺) medium for 24 h in closed container and were immunostained with antibodies to 8-hydroxydeoxyguanosine (8-OH-dG) or 4-hydroxy-2-nonenal (4-HNE). Insets: high-magnification views of areas in the rectangles. Arrows indicate increased signals in cytoplasmic regions. DAPI, 4',6-diamidino-2-phenylindole. Scale bars = 50 μ m. B and D: fluorescent signals in response to 8-OH-dG or 4-HNE were quantified with 100 cells from each independent experiment ($n = 5$). E: propidium iodide (PI, dead cells) or Hoechst 33342 (nuclei) staining of irradiated cells after a 36-h incubation in N₂-rich (H₂⁻) or H₂-rich (H₂⁺) medium in tightly closed containers filled with H₂-rich or N₂-rich mixed gases. Insets: high-magnification views of areas in the rectangles. Arrows indicate dead cells. Scale bars = 50 μ m. F: cell survival, shown as the ratio PI/Hoechst-positive cells, was assessed by manual counting ($n = 5$). Data represent means \pm SE. * $P < 0.05$ and ** $P < 0.01$.

During regulation of the apoptotic response, mammalian cells use prosurvival proteins from the Bcl-2 family that antagonize the proapoptotic function of Bax (42). Bax translocation from the cytosol to mitochondria is a critical step in the triggering of death signals (50), which leads to cytochrome

c release and activates caspase 9, which then activates caspase 3 (42). Caspase 3 activation is essential for cleavage of the DNA repair enzyme poly(ADP-ribose) polymerase, which results in genomic DNA fragmentation as an apoptotic reaction. Upregulation of Bax and activation of caspase 3 are reportedly

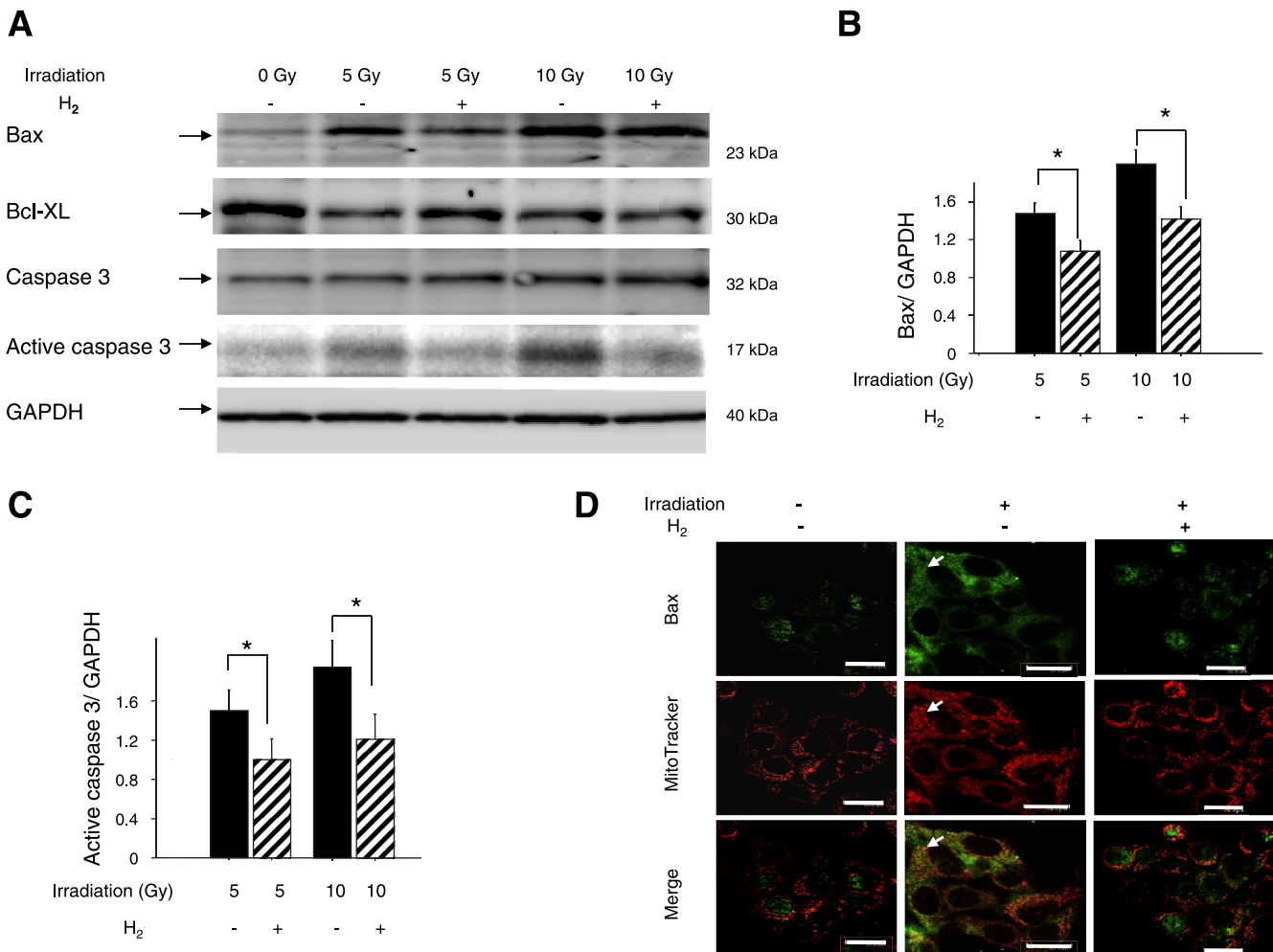


Fig. 3. Effects of H₂ on modulation of apoptotic marker proteins in irradiated cells. **A**: after a 24-h incubation of irradiated cells (0, 5, or 10 Gy) in N₂-rich (H₂⁻) or H₂-rich (H₂⁺) medium in tightly closed containers filled with H₂-rich or N₂-rich mixed gases, cell extracts (lysates) were subjected to 10% SDS-PAGE and were immunoblotted with antibodies against Bax, Bcl-x_L, caspase 3, active caspase 3, and GAPDH (control). **B** and **C**: in 5 experiments similar to that whose results appear in **A**, amounts of each protein were quantified by densitometry and expressed relative to the amount of GAPDH in the same samples. Results are reported relative to those of 5 nonirradiated controls in 5 experiments (no irradiation = 1.0). Data represent means \pm SE. **D**: representative images of fluorescence of Bax (green), MitoTracker (mitochondria; red), and merged images taken 24 h after irradiation. Arrows indicate colocalization (yellow) of positive findings for Bax and MitoTracker as mitochondrial translocation. Scale bars = 20 μ m. **P* < 0.05.

induced by ionizing irradiation as markers of an apoptotic response (41, 50).

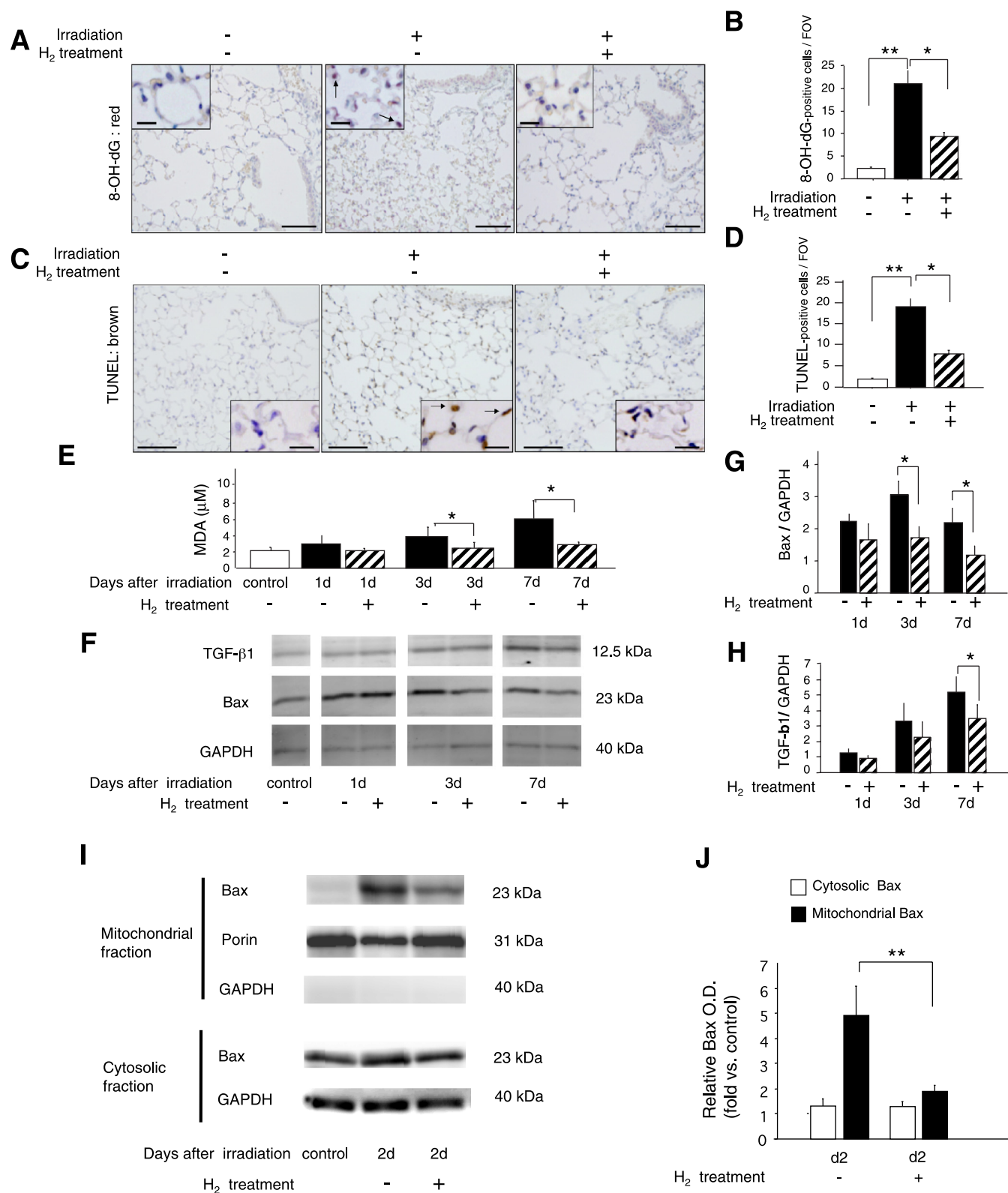
In our investigations reported here, we showed that H₂ effectively suppressed cell death, as seen with propidium iodide/Hoechst staining (Fig. 2, *E* and *F*), by decreasing apoptotic events, such as upregulation of Bax associated with translocation from the cytosol to mitochondria and activation of caspase 3 (Fig. 3), via preservation of cellular oxidative status as shown by levels of 8-OH-dG (DNA oxidation) and 4-HNE (lipid peroxidation) (Fig. 2, *A–D*). Clear suppression of damage indicates that H₂ prevented deterioration of the bioenergetic state of cells caused by irradiation in vitro. These findings are consistent with a report of inhibition of radiation-induced apoptosis in human Molt-4 cells by antioxidants such as *N*-acetyl-L-cysteine and Trolox (6-hydroxy-2,5,7,8-tetramethylchroman-2-carboxylic acid, a water-soluble derivative of vitamin E) (30). Data from our study thus suggest that H₂ can scavenge ROS and

protect against apoptotic damage related to oxidative stress induced by irradiation in vitro.

Radiation-induced lung injury is characterized by an acute pneumonitic phase that is followed by a fibrotic phase that develops months or years after irradiation (25). Previous investigations supported the idea that oxidative stress initiates and maintains radiation-induced lung injury in vivo (10, 22, 24). In addition to producing a rapid, short-lived burst of ROS at the time of irradiation, stimulation of local ROS-generating systems, such as NADPH oxidase, xanthine oxidase, nitric oxide synthase (NOS), and the dysfunctional mitochondrial respiratory chain, have causative implications for development of chronic radiation-induced lung injury because of the resulting excess of ROS such as H₂O₂, O₂^{•-}, ONOO⁻, and [•]OH (10, 21–24, 26). In fact, ROS directly or indirectly regulate several transcription factors (such as nuclear factor- κ B and hypoxia-inducible factor-1 α) and their downstream products (such as TGF- β and vascular endothelial growth factor) (23). Thus both

the short-lived burst of ROS and the sustained local ROS concentration have causative roles in acute and late radiation-induced lung damage and are therefore extremely important targets in protection from irradiation-induced oxidative stress in vivo.

Our in vitro data showed that H₂ treatment can scavenge ROS and protect against apoptotic damage related to oxidative stress induced by irradiation, but H₂ treatment did not completely scavenge ROS and could not fully protect against apoptotic damage induced by irradiation (Figs. 1–3). There-



fore, in our *in vivo* study reported here, we used inhalation of H_2 gas during irradiation for protection against the short-lived burst of ROS that causes acute damage, as well as continuous access to H_2 -rich drinking water, up to the late damage phase, for protection against continuing oxidative damage from sustained local ROS concentrations. This treatment design was based on the specific pathophysiological mechanism of lung late damage from irradiation *in vivo*. We found that H_2 treatment was indeed radioprotective not only *in vitro* but also *in vivo*.

H_2 treatment significantly reduced the severity of the ionizing radiation-induced oxidative injury and the apoptotic response in mouse lungs, as evidenced by levels of MDA, 8-OH-dG, TUNEL, Bax, and Bax mitochondrial translocation, and reduced TGF- β 1 expression (Fig. 4) during the acute damage phase. These results are similar to previous findings of protection of the brain, heart, and liver from acute oxidative stress injury by means of inhalation of 1% H_2 gas, whose concentration in blood was estimated as 8 μ M (12, 16, 32). This protection may have been mainly due to ROS (\cdot OH and ONOO $^-$) scavenging by H_2 , as our *in vitro* results suggested.

We also determined, by means of chest micro-CT and pathological findings, that the radioprotective effects of our H_2 treatment, as reflected by suppression of lung fibrosis, were evident 5 mo after exposure to irradiation, during the late phase of damage (Fig. 5). One study of a nephrotoxic model in mice reported that H_2 detected in blood after mice drank water containing H_2 reached a concentration of several μ M in 3 min and led to reduced oxidative stress (29). Therefore, continuous exposure to H_2 by drinking H_2 -rich water may maintain, via blood circulation, protection against the sustained oxidative state of the irradiated lung, although H_2 obtained by drinking H_2 -rich water is thought to be retained for a relatively short period and at a low concentration. Because H_2 is expired via the lung, a metabolic organ with a large pulmonary blood flow, and H_2 can spread quickly into cells in the lung because of the loose anatomical structure of the lung, H_2 can easily reach lung cells. Other studies have reported results similar to ours, that continuous drinking of H_2 -rich water may protect against persisting oxidative damage, such as atherosclerosis in apolipoprotein E knockout mice for 6-mo treatment (33), indications of oxidative stress in patients with diabetes for 8-wk treatment (19), cisplatin-induced renal injury in mice for 10-day treatment (29), and chronic allograft nephropathy in rats for 5-mo treatment (6). Our results for protection during the late phase of irradiation damage may result partly from the protective effect

of scavenging ROS (\cdot OH and ONOO $^-$) during the acute damage phase that was achieved by H_2 inhalation and partly from the protective effect of scavenging ROS that was obtained by drinking H_2 -rich water during the late damage phase, which involves sustained local oxidative stress from relatively reactive ROS such as H_2O_2 , $O_2^{\cdot-}$, and ONOO $^-$.

ONOO $^-$, as assessed by nitrotyrosine production, was reportedly a local ROS, formed from $O_2^{\cdot-}$ and NO, whose production was sustained in irradiation-induced injury of the lung and salivary gland; inhibition of NOS prevented these irradiation-induced injuries (13, 15, 44). Because H_2 also reduced ONOO $^-$, we suggest that H_2 treatment including drinking H_2 -rich water may also have the protective effect of scavenging ONOO $^-$ during late damage phases in our irradiation model in addition to during acute damage phases.

Certain reports indicated that H_2O_2 and $O_2^{\cdot-}$ play critical roles in the process of radiation-induced lung injury as a short-lived burst of ROS and sustained local ROS, with the evidence of protective effect by using several kinds of SOD-related treatments (1, 24). Drinking H_2 -rich water was recently reported to have a protective effect through reduction of oxidative stress associated with upregulation of SOD activity, for example, in subjects with metabolic syndrome after 8 wk of H_2 treatment (28) and in senescence-accelerated prone SAMP8 mice, which have a higher oxidative stress status with mitochondrial dysfunction, after 18 wk of H_2 treatment (14). Thus the precise mechanisms of the protective effect of drinking H_2 -rich water are still under investigation. However, we suggest that drinking H_2 -rich water may have protective effects against H_2O_2 and $O_2^{\cdot-}$ during the late damage phase in our model through upregulated SOD activity.

A wide variety of antioxidants, including thiol compounds and natural antioxidants and extracts, reportedly protect against radiation toxicity (45, 49). Thiol compounds are the most effective and the longest studied radioprotectors. The synthetic thiol amifostine is the only U.S. Food and Drug Administration-approved radioprotectant available today (8). However, it has critical weaknesses, such as relatively high toxicity, unfavorable routes of administration, and a short protection period (17). Natural antioxidants, such as vitamin E, melatonin, flavonoids, and others, have fewer toxic side effects but also offer less protection compared with thiol agents (17, 48).

Compared with these antioxidants, H_2 has the advantage of protecting cells without clearly affecting $O_2^{\cdot-}$ and H_2O_2 , which have important physiological roles. If too much H_2 is taken in, the excess would be expired via the lungs. In fact, H_2

Fig. 4. Reduced irradiation-induced acute lung damage in mice by H_2 treatment. C57BL/6J female mice received a single dose of 15 Gy to the thorax. H_2 treatment groups inhaled a mixture of 3% H_2 and 97% air during the 90-min irradiation and recovery period and continuously drank H_2 water ad libitum after irradiation until each evaluation stage. The no- H_2 treatment groups inhaled a mixture of 3% N_2 and 97% air during irradiation and drank water without H_2 . A and C: on day 1 after irradiation, paraffin-embedded lung sections from each group were stained with 8-OH-dG antibody (A) or terminal deoxynucleotidyl transferase dUTP nick end-labeling (TUNEL) (C). Insets: high-magnification views. Arrows indicate positive findings. Scale bars = 100 μ m, and 15 μ m for insets (high magnification). B and D: the number of cells positive for 8-OH-dG or TUNEL, per field of view (FOV), were counted in areas of the same size from lungs of each group ($n = 6$). E: lung tissue extracts from irradiated mice that had H_2 treatment or no treatment were analyzed for levels of free malondialdehyde (MDA), a marker of oxidative stress, with normalization to protein contents in extracts. F and I: total lung tissue extracts or lung tissue extracts separated into cytosolic and mitochondrial fractions were also subjected to SDS-PAGE and were immunoblotted with antibodies against Bax, transforming growth factor (TGF)- β 1, GAPDH (total or cytosolic loading control), and porin (mitochondrial loading control). F: representative blots with spaces provide control and days 1 and 3 and 7 results with and without H_2 treatment, respectively, obtained from a blotting experiment performed on the same day under the same condition. G, H, and J: in 6 experiments similar to that whose results appear in F and I, amounts of each protein were quantified by densitometry and expressed relative to the amount of GAPDH or porin in the same samples. Results are reported relative to those of 6 nonirradiated controls in 6 experiments (no irradiation = 1.0). Data represent means \pm SE. * $P < 0.05$ and ** $P < 0.01$.

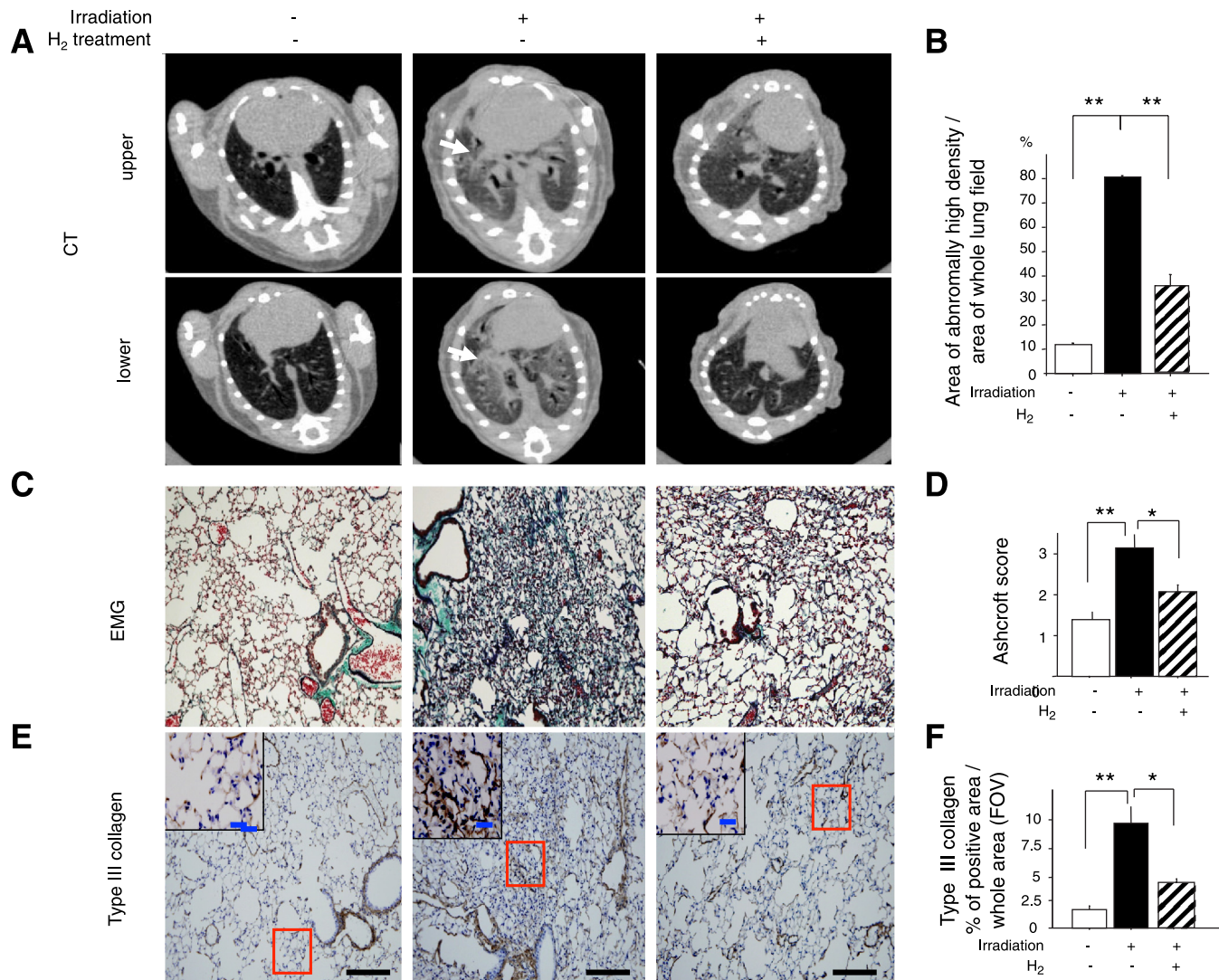


Fig. 5. Reduced irradiation-induced lung fibrosis (late lung damage) in mice by H₂ treatment. **A**: micro-computed tomography (CT) axial sections show the middle (*top*) and lower (*bottom*) thoracic areas from control and irradiated mice at 5 mo after whole thorax irradiation. Irradiated mice showed a regional increase in radioopaque lesions (arrows), but mice receiving H₂ treatment had a lower increase. **B**: ratios of areas of abnormally high density to whole lung fields in the same slice were calculated and compared for nonirradiated and irradiated lungs with or without H₂ treatment ($n = 5$). **C** and **E**: at 5 mo after irradiation, lung sections for each group were stained with hematoxylin and eosin and elastica Masson-Goldner (EMG) (**C**) or with antibody to type III collagen (**E**). *Insets*: high-magnification views of areas in the rectangles. Scale bars = 100 μ m, and 20 μ m for insets (high magnification). **D** and **F**: severity of lung fibrosis was evaluated with the Ashcroft score (**D**), and areas positive for collagen III (**F**) per FOV were analyzed for the areas of the same size from lungs of each group ($n = 6$). Data represent means \pm SE. * $P < 0.05$ and ** $P < 0.01$.

has already been used for humans, to prevent decompression sickness in divers, at a level of 2 MPa partial pressure of H₂, which suggests that 16 mM H₂ in blood may be a safe level (11). Previous investigations reported that, in cases of acute and severe oxidative stress induced by ischemia-reperfusion, 1% H₂ gas was sufficient for protection, without influencing physiological characteristics such as body temperature, blood pressure, pH, and blood Po₂ (5, 12, 16, 32). In addition to inhaling H₂ gas, drinking H₂-rich water would protect against continuing oxidative damage, as mentioned before (19). Of course, drinking H₂-rich water as a method of H₂ treatment has an advantage of convenience.

Thus, in our study, H₂, supplied at the onset of irradiation by the inhalation of H₂ gas and during the period after irradiation

by the drinking of H₂-rich water, may have direct and indirect influences as protection against the oxidative state of the lung and may lead to suppression of irradiation-induced fibrosis. Although our data cannot separate the effects of inhaling H₂ gas and drinking H₂-rich water, we were able to provide evidence of the radioprotective effect of H₂ treatment against acute and late radiation-induced lung damage *in vivo*, which we believe is the first report of such evidence.

In conclusion, we showed here that H₂, with no known toxic side effects, effectively protects cells and lungs of mice from oxidative stress and damage caused by irradiation because of the rapid diffusion of H₂ across cell membranes and its reaction with cytotoxic ROS. Thus development of H₂-related antioxidant approaches to treatment of lung damage caused by irra-

diation may be possible and may also provide protection against irradiation-induced interstitial pneumonitis.

ACKNOWLEDGMENTS

The authors thank Ms. Judith B. Gandy for excellent editing of the manuscript.

GRANTS

This study was supported by Grants-in-Aid for Scientific Research from the Ministry of Education, Culture, Sports, Science and Technology (MEXT) of Japan. This study was also partly supported by a grant to the Diffuse Lung Diseases Research Group from the Ministry of Health, Labor and Welfare of Japan.

DISCLOSURES

No conflicts of interest, financial or otherwise, are declared by the authors.

REFERENCES

1. Anscher MS, Chen L, Rabbani Z, Kang S, Larrier N, Huang H, Samulski TV, Dewhirst MW, Brizel DM, Folz RJ, Vujaskovic Z. Recent progress in defining mechanisms and potential targets for prevention of normal tissue injury after radiation therapy. *Int J Radiat Oncol Biol Phys* 62: 255–259, 2005.
2. Ashcroft T, Simpson JM, Timbrell V. Simple method of estimating severity of pulmonary fibrosis on a numerical scale. *J Clin Pathol* 41: 467–470, 1988.
3. Beyzadeoglu M, Oysul K, Dirican B, Arpacı F, Balkan A, Surenkok S, Pak Y. Effect of dose-rate and lung dose in total body irradiation on interstitial pneumonitis after bone marrow transplantation. *Tohoku J Exp Med* 202: 255–263, 2004.
4. Brown WR, Isobe Y, Nakane PK. Studies on translocation of immunoglobulins across intestinal epithelium. II. Immunoelectron-microscopic localization of immunoglobulins and secretory component in human intestinal mucosa. *Gastroenterology* 71: 985–995, 1976.
5. Buchholz BM, Kaczorowski DJ, Sugimoto R, Yang R, Wang Y, Billiar TR, McCurry KR, Bauer AJ, Nakao A. Hydrogen inhalation ameliorates oxidative stress in transplantation induced intestinal graft injury. *Am J Transplant* 8: 2015–2024, 2008.
6. Cardinal JS, Zhan J, Wang Y, Sugimoto R, Tsung A, McCurry KR, Billiar TR, Nakao A. Oral hydrogen water prevents chronic allograft nephropathy in rats. *Kidney Int* 77: 101–109, 2010.
7. Carruthers SA, Wallington MM. Total body irradiation and pneumonitis risk: a review of outcomes. *Br J Cancer* 90: 2080–2084, 2004.
8. Cassatt DR, Fazenbaker CA, Bachy CM, Hanson MS. Preclinical modeling of improved amifostine (Ethyol) use in radiation therapy. *Semin Radiat Oncol* 12: 97–102, 2002.
9. Deeg HJ. Acute and delayed toxicities of total body irradiation. Seattle Marrow Transplant Team. *Int J Radiat Oncol Biol Phys* 9: 1933–1939, 1983.
10. Fleckenstein K, Zgonjanin L, Chen L, Rabbani Z, Jackson IL, Thrasher B, Kirkpatrick J, Foster WM, Vujaskovic Z. Temporal onset of hypoxia and oxidative stress after pulmonary irradiation. *Int J Radiat Oncol Biol Phys* 68: 196–204, 2007.
11. Fontanari P, Badier M, Guillot C, Tomei C, Burnet H, Gardette B, Jammes Y. Changes in maximal performance of inspiratory and skeletal muscles during and after the 7.1-MPa Hydra 10 record human dive. *Eur J Appl Physiol* 81: 325–328, 2000.
12. Fukuda K, Asoh S, Ishikawa M, Yamamoto Y, Ohsawa I, Ohta S. Inhalation of hydrogen gas suppresses hepatic injury caused by ischemia/reperfusion through reducing oxidative stress. *Biochem Biophys Res Commun* 361: 670–674, 2007.
13. Gaiad A, Lehnert SM, Chehayeb B, Chehayeb D, Kaplan I, Shenouda G. Inducible nitric oxide synthase and nitrotyrosine in mice with radiation-induced lung damage. *Am J Clin Oncol* 26: e67–e72, 2003.
14. Gu Y, Huang CS, Inoue T, Yamashita T, Ishida T, Kang KM, Nakao A. Drinking hydrogen water ameliorated cognitive impairment in senescence-accelerated mice. *J Clin Biochem Nutr* 46: 269–276, 2010.
15. Hanaue N, Takeda I, Kizu Y, Tonogi M, Yamane GY. Peroxynitrite formation in radiation-induced salivary gland dysfunction in mice. *Biomed Res (Tokyo)* 28: 147–151, 2007.
16. Hayashida K, Sano M, Ohsawa I, Shinmura K, Tamaki K, Kimura K, Endo J, Katayama T, Kawamura A, Kohsaka S, Makino S, Ohta S, Ogawa S, Fukuda K. Inhalation of hydrogen gas reduces infarct size in the rat model of myocardial ischemia-reperfusion injury. *Biochem Biophys Res Commun* 373: 30–35, 2008.
17. Hosseinimehr SJ. Trends in the development of radioprotective agents. *Drug Discov Today* 12: 794–805, 2007.
18. Jackson IL, Vujaskovic Z, Down JD. Revisiting strain-related differences in radiation sensitivity of the mouse lung: recognizing and avoiding the confounding effects of pleural effusions. *Radiat Res* 173: 10–20, 2010.
19. Kajiya S, Hasegawa G, Asano M, Hosoda H, Fukui M, Nakamura N, Kitawaki J, Imai S, Nakano K, Ohta M, Adachi T, Obayashi H, Yoshikawa T. Supplementation of hydrogen-rich water improves lipid and glucose metabolism in patients with type 2 diabetes or impaired glucose tolerance. *Nutr Res* 28: 137–143, 2008.
20. Kawakami M, Matsuo Y, Yoshiura K, Nagase T, Yamashita N. Sequential and quantitative analysis of a murine model of elastase-induced emphysema. *Biol Pharm Bull* 31: 1434–1438, 2008.
21. Leach JK, Van Tuyle G, Lin PS, Schmidt-Ullrich R, Mikkelsen RB. Ionizing radiation-induced, mitochondria-dependent generation of reactive oxygen/nitrogen. *Cancer Res* 61: 3894–3901, 2001.
22. Lee JC, Krochak R, Blouin A, Kanterakis S, Chatterjee S, Arguiri E, Vachani A, Solomides CC, Cengel KA, Christofidou-Solomidou M. Dietary flaxseed prevents radiation-induced oxidative lung damage, inflammation and fibrosis in a mouse model of thoracic radiation injury. *Cancer Biol Ther* 8: 47–53, 2009.
23. Li F, Sonveaux P, Rabbani ZN, Liu S, Yan B, Huang Q, Vujaskovic Z, Dewhirst MW, Li CY. Regulation of HIF-1 α stability through S-nitrosylation. *Mol Cell* 26: 63–74, 2007.
24. Machtay M, Scherpereel A, Santiago J, Lee J, McDonough J, Kinniry P, Arguiri E, Shuvaev VV, Sun J, Cengel K, Solomides CC, Christofidou-Solomidou M. Systemic polyethylene glycol-modified (PEGylated) superoxide dismutase and catalase mixture attenuates radiation pulmonary fibrosis in the C57/bl6 mouse. *Radiother Oncol* 81: 196–205, 2006.
25. McDonald S, Rubin P, Phillips TL, Marks LB. Injury to the lung from cancer therapy: clinical syndromes, measurable endpoints, and potential scoring systems. *Int J Radiat Oncol Biol Phys* 31: 1187–1203, 1995.
26. Mikkelsen RB, Wardman P. Biological chemistry of reactive oxygen and nitrogen and radiation-induced signal transduction mechanisms. *Oncogene* 22: 5734–5754, 2003.
27. Mizuguchi M, Sohma O, Takashima S, Ikeda K, Yamada M, Shiraiwa N, Ohta S. Immunohistochemical and immunohistochemical localization of Bcl-x protein in the rat central nervous system. *Brain Res* 712: 281–286, 1996.
28. Nakao A, Toyoda Y, Sharma P, Evans M, Guthrie N. Effectiveness of hydrogen rich water on antioxidant status of subjects with potential metabolic syndrome—an open label pilot study. *J Clin Biochem Nutr* 46: 140–149, 2010.
29. Nakashima-Kamimura N, Mori T, Ohsawa I, Asoh S, Ohta S. Molecular hydrogen alleviates nephrotoxicity induced by an anti-cancer drug cisplatin without compromising anti-tumor activity in mice. *Cancer Chemother Pharmacol* 64: 753–761, 2009.
30. Ogura A, Oowada S, Kon Y, Hirayama A, Yasui H, Meike S, Kobayashi S, Kuwabara M, Inanami O. Redox regulation in radiation-induced cytochrome c release from mitochondria of human lung carcinoma A549 cells. *Cancer Lett* 277: 64–71, 2009.
31. Oharazawa H, Igarashi T, Yokota T, Fujii H, Suzuki H, Machide M, Takahashi H, Ohta S, Ohsawa I. Protection of the retina by rapid diffusion of hydrogen: administration of hydrogen-loaded eye drops in retinal ischemia-reperfusion injury. *Invest Ophthalmol Vis Sci* 51: 487–492, 2010.
32. Ohsawa I, Ishikawa M, Takahashi K, Watanabe M, Nishimaki K, Yamagata K, Katsura K, Katayama Y, Asoh S, Ohta S. Hydrogen acts as a therapeutic antioxidant by selectively reducing cytotoxic oxygen radicals. *Nat Med* 13: 688–694, 2007.
33. Ohsawa I, Nishimaki K, Yamagata K, Ishikawa M, Ohta S. Consumption of hydrogen water prevents atherosclerosis in apolipoprotein E knockout mice. *Biochem Biophys Res Commun* 377: 1195–1198, 2008.
34. Para AE, Bezjak A, Yeung IW, Van Dyk J, Hill RP. Effects of genistein following fractionated lung irradiation in mice. *Radiother Oncol* 92: 500–510, 2009.
35. Qian L, Cao F, Cui J, Huang Y, Zhou X, Liu S, Cai J. Radioprotective effect of hydrogen in cultured cells and mice. *Free Radic Res* 44: 275–282, 2010.

36. **Riley PA.** Free radicals in biology: oxidative stress and the effects of ionizing radiation. *Int J Radiat Biol* 65: 27–33, 1994.
37. **Sampath S, Schultheiss TE, Wong J.** Dose response and factors related to interstitial pneumonitis after bone marrow transplant. *Int J Radiat Oncol Biol Phys* 63: 876–884, 2005.
38. **Shirazi A, Ghobadi G, Ghazi-Khansari M.** A radiobiological review on melatonin: a novel radioprotector. *J Radiat Res (Tokyo)* 48: 263–272, 2007.
39. **Spitz DR, Azzam EI, Li JJ, Gius D.** Metabolic oxidation/reduction reactions and cellular responses to ionizing radiation: a unifying concept in stress response biology. *Cancer Metastasis Rev* 23: 311–322, 2004.
40. **Sun Y, Sun D, Li F, Tian L, Li C, Li L, Lin R, Wang S.** Downregulation of Sirt1 by antisense oligonucleotides induces apoptosis and enhances radiation sensitization in A549 lung cancer cells. *Lung Cancer* 58: 21–29, 2007.
41. **Tak JK, Park JW.** The use of ebselen for radioprotection in cultured cells and mice. *Free Radic Biol Med* 46: 1177–1185, 2009.
42. **Thotala DK, Geng L, Dickey AK, Hallahan DE, Yazlovitskaya EM.** A new class of molecular targeted radioprotectors: GSK-3beta inhibitors. *Int J Radiat Oncol Biol Phys* 76: 557–565.
43. **Tomizawa S, Imai H, Tsukada S, Simizu T, Honda F, Nakamura M, Nagano T, Urano Y, Matsuoka Y, Fukasaku N, Saito N.** The detection and quantification of highly reactive oxygen species using the novel HPF fluorescence probe in a rat model of focal cerebral ischemia. *Neurosci Res* 53: 304–313, 2005.
44. **Tsuji C, Shioya S, Hirota Y, Fukuyama N, Kurita D, Tanigaki T, Ohta Y, Nakazawa H.** Increased production of nitrotyrosine in lung tissue of rats with radiation-induced acute lung injury. *Am J Physiol Lung Cell Mol Physiol* 278: L719–L725, 2000.
45. **Vijayalaxmi Reiter RJ, Tan DX, Herman TS, Thomas CR Jr.** Melatonin as a radioprotective agent: a review. *Int J Radiat Oncol Biol Phys* 59: 639–653, 2004.
46. **Ward JF.** DNA damage produced by ionizing radiation in mammalian cells: identities, mechanisms of formation, and reparability. *Prog Nucleic Acid Res Mol Biol* 35: 95–125, 1988.
47. **Weiner RS, Bortin MM, Gale RP, Gluckman E, Kay HE, Kolb HJ, Hartz AJ, Rimm AA.** Interstitial pneumonitis after bone marrow transplantation. Assessment of risk factors. *Ann Intern Med* 104: 168–175, 1986.
48. **Weiss JF, Landauer MR.** Protection against ionizing radiation by antioxidant nutrients and phytochemicals. *Toxicology* 189: 1–20, 2003.
49. **Weiss JF, Landauer MR.** Radioprotection by antioxidants. *Ann NY Acad Sci* 899: 44–60, 2000.
50. **Zhang Y, Xing D, Liu L.** PUMA promotes Bax translocation by both directly interacting with Bax and by competitive binding to Bcl-X L during UV-induced apoptosis. *Mol Biol Cell* 20: 3077–3087, 2009.
51. **Zhao W, Robbins ME.** Inflammation and chronic oxidative stress in radiation-induced late normal tissue injury: therapeutic implications. *Curr Med Chem* 16: 130–143, 2009.

